# The impact of sea breezes on offshore wind energy resources in Australia

Andrew Brown[1,2] and Claire Vincent[1,2]

[1]ARC Centre of Excellence for 21st Century Weather, The University of Melbourne, Australia
[2]School of Geography, Earth and Atmospheric Sciences, The University of Melbourne, Australia

**Correspondence:** Andrew Brown (a.brown1@unimelb.edu.au)

**Abstract.**

Future projected increases in offshore wind energy in Australia means that it is important to understand variability in wind resources. This includes the potential diurnal variation of wind, and its co-variability with known diurnal variations of energy demand and supply. A key mechanism for diurnal variations in coastal near-surface winds is the sea breeze, which is driven by differential land-sea surface heating during the day. Here, a new dataset characterising the sea breeze as a frontal object, derived from a km-scale reanalysis, is used to analyse the impact of the sea breeze on diurnal variations of wind energy resources over 1979–2024. This analysis is performed over eight potential offshore wind areas in southeastern and southwestern Australia during the summer. On days with a sea breeze object, there tends to be more potential wind energy resources available in coastal and offshore wind areas during the afternoon, although there may also be late-morning lulls due to the sea breeze opposing the existing prevailing winds. In addition, days with a sea breeze correspond to higher regional energy demand on average, due to warmer air temperatures over the land, while the peak in potential wind energy occurs with similar timing to peak demand. Finally, due to the role of the prevailing wind direction in sea breeze formation, there is an anti-correlation in occurrences between opposite-facing coastlines. These results have implications for energy system planning and suggest that offshore wind farm development on a diverse set of coastlines should be encouraged in Australia.

## 1 Introduction

Global offshore wind energy is growing rapidly, with 83 GW of installed capacity as of 2024 (Global Wind Energy Council, 2025). Although there are currently no offshore wind farms operational in Australia, it is projected to grow into the future, with Australian state government targets of 9 GW by 2050 (Australian Energy Market Operator, 2024). To help understand the potential impacts on energy system reliability, it is important to understand variability in wind resources in offshore coastal areas. Wind energy resources in Australia can vary on a range of time scales, from diurnal to multi-year (Vincent and Dowdy, 2024), including periods of low wind that could lead to potential shortfalls in supply (Richardson et al., 2023). Diurnal variations in wind energy resources are particularly important, given there are also large diurnal variations in both energy demand and existing supply (for example, Mulder, 2014; Simshauser and Wild, 2025). Previous studies have suggested that diurnal wind variations could align well with diurnal peaks in energy demand (Pickering et al., 2020; Vincent et al., 2025).

In coastal areas, the sea breeze is a dominant mode of diurnal wind variability. It is the result of differential surface heating between the land and sea during the day, and is often described as a thermally-direct circulation, which has an onshore surface branch with rising air over the land, and an offshore branch aloft with descending air over the sea (Markowski and Richardson, 2010). The differential surface temperature forcing can also be influenced by small-scale variations in land-use types, such as due to the presence of cities along the coastline (Wang et al., 2017). The onshore surface branch of the sea breeze tends to form a front ahead of the maritime air mass (the sea breeze front) that can propagate several hundreds of kilometres onshore as a density current (Clarke, 1983; Simpson, 1999; Bao et al., 2023). Meanwhile, the sea breeze circulation can influence the offshore surface wind field, and this has been shown to impact offshore wind energy potential in several regions already, including in the North Sea (Steele et al., 2015) and the United States (Xia et al., 2022). In regions equator-ward of 30° latitude, the offshore extent of the sea breeze system can also be influenced by inertia-gravity waves that propagate away from the region of diurnal coastal heating (Rotunno, 1983; Short et al., 2019).

Sea breeze occurrences and their intensity can also be influenced by the prevailing background wind conditions. For example, prevailing onshore winds are typically considered to be unfavourable for sea breeze formation (Frysinger et al., 2003; Masouleh et al., 2019; Xia et al., 2022). Sea breezes have been observed to occur in such conditions, but with a weaker front (Reible et al., 1993). In contrast, along-shore prevailing winds with the land to the right (in the Southern Hemisphere) can lead to "corkscrew" sea breezes, and prevailing winds with the land to the left can lead to "backdoor" sea breezes (Miller et al., 2003, with the inverse occurring in the Northern Hemisphere). Corkscrew sea breezes are often observed to have stronger surface wind speeds compared with backdoor sea breezes, as well as so-called "pure" sea breezes that occur with prevailing winds that are directly offshore (Steele et al., 2015). Miller et al. (2003) suggest that corkscrew sea breezes are more intense due to the gradient in surface friction over land and sea surfaces. This creates differential and divergent ageostrophic wind components over the land and sea, towards synoptic-scale low pressure regions (to the right in the southern hemisphere), both acting in the same direction as the onshore sea breeze flow. Steele et al. (2015) demonstrated that these different sea breeze types can have varying impacts on offshore wind energy potential. In addition, the prevailing wind speed and direction has been shown to influence the offshore and onshore extent of the sea breeze (Arritt, 1989; Rafiq et al., 2020; Finocchio et al., 2025).

Here, we investigate the impact of sea breezes on the diurnal cycle of wind energy resources for several potential offshore wind areas in southeastern and southwestern Australia. This is done using a new dataset of sea breeze objects derived from an atmospheric reanalysis, based on a diagnostic of sea breeze fronts presented by Brown et al. (2025b). Typically, previous studies have identified sea breezes for individual coastal sites based on local characteristics, with the approach here representing a more general and robust method for detection, allowing for consistent analysis over a broader region. Sea breeze objects are derived from a km-scale atmospheric reanalysis over Australia for a 46-year period. These km-scale models are able to more accurately resolve mesoscale sea breeze processes over complex coastlines, compared with coarser models that are more suited for representing the large-scale processes conducive to sea breeze formation (Bergemann et al., 2017; Cafaro et al., 2019).

Sea breeze objects are used to investigate the seasonal cycle and spatial distribution of sea breezes over the broad region of southwest and southeast Australia. Then, the diurnal cycle of wind energy capacity factors are calculated over specific wind energy regions for days with a sea breeze object, and are compared with other days, to quantify the wind resource associated

60 with the sea breeze. For simplicity, the latter analysis is presented for the Austral summer period (December–February), given that this time of year is when sea breezes are more likely to occur due to relatively intense daytime heating of the land. The diurnal cycle in wind energy is compared with regional energy demand for each offshore wind area, as a qualitative assessment of the value of the potential energy resource related to sea breezes. In addition, we also consider the co-variability of sea breezes across different offshore wind zones, as an important consideration for optimising energy systems (Gunn et al., 2023).

## 2 Data and methods

### 2.1 Sea breeze objects

A frontogenesis method is used as a diagnostic of sea breeze fronts from atmospheric model output, following a method outlined by Brown et al. (2025b). Diagnostics of frontogenesis can identify areas of growth in the frontal boundary between relatively cool, moist maritime air and dry, warm terrestrial air. (Keyser et al., 1988; Kraus et al., 1990). Positive frontogenesis

70 values indicate regions where the gradient in a scalar quantity is increasing due to deformation in the horizontal flow. In the case of sea breezes, specific humidity ($q$) is chosen as the scalar quantity, referred to as "moisture frontogenesis". The frontogenesis formulation is in the form of Pettersen (1956):

$$F = \frac{1}{2}|\nabla_h q|[D_{total} \times cos(2B) - \delta] \tag{1}$$

where $D_{total}$ is the total deformation of the surface wind field, $B$ is the angle between the axis of dilatation (the axis along

75 which the stretching of the air is most rapid) and the isopleths of $q$, and $\delta$ is the divergence of the surface wind field. Deformation is defined as $D_{total} = \sqrt{D_{stretch}^2 + D_{shear}^2}$, where $D_{stretch} = du/dx - dv/dy$ is the stretching deformation and $D_{shear} = dv/dx + du/dy$ is the shearing deformation.

The sea breeze identification method consists of calculating the moisture frontogenesis diagnostic using hourly data over 1979–2024, from the Bureau of Meteorology Atmospheric Regional Reanalysis for Australia version 2 (BARRA2, Su et al.,

80 2025). The BARRA2 reanalysis system includes a regional model run over the broader Australasia region with 12 km horizontal grid spacing (BARRA-R2) and a downscaled model run over Australia with 4.4 km horizontal grid spacing (BARRA-C2). BARRA-C2 is used here to sufficiently capture the sea breeze. However, following Brown et al. (2025b), a Gaussian smoothing filter is applied to BARRA-C2 data in the spatial dimension before calculating frontogenesis, to remove small-scale moisture gradients.

85 For calculating frontogenesis, 10 m $u$ and $v$ winds are used, as well as surface specific humidity (at a height of 1.5 m). A mask of candidate sea breeze objects is then created by taking exceedances of frontogenesis over a threshold value of 16.1 g/kg/100 km/3h, following Brown et al. (2025b), before a series of filters are applied intended to remove non-sea-breeze fronts. These filters include conditions on the morphology of the objects, as well as constraints on object-averaged physical variables. For further details on these methods, including the smoothing and pre-processing of model fields, the reader is referred to Brown

90 et al. (2025b).

An additional sea breeze filtering step is developed and applied in this study, compared with the method of Brown et al. (2025b). That is, the change in specific humidity relative to the previous hour, averaged spatially over the candidate sea breeze object, must be positive. This is intended to remove synoptic-scale cold fronts, which are dry, and occur frequently over southern Australia during the cool season. The application of this filter did not significantly change the total spatial distribution
95 of object occurrences, but did lower the amount of sea breeze objects during the winter, likely related to a reduction in the mis-classification of synoptic-scale cold fronts (not shown).

As a way of evaluating the sea breeze identification method, we have compared the seasonal cycle in "sea breeze front days" (see Section 2.2 for definition) with three previous studies in different regions of Australia (Masselink and Pattiaratchi, 2001; Pazandeh Masouleh et al., 2016; Soderholm et al., 2017). These comparisons are shown in Section S1 of the Supplementary
100 Material. The number of sea breeze front days defined using the methods here are similar to these previous studies, with a broadly similar seasonal cycle, despite the very different methods and periods used. This provides confidence in the use of the methods described here.

However, it should be kept in mind that mis-classification of other fronts and circulations as sea breezes are possible. This includes convective cold pools, up-slope mountain flows, frictional convergence at the coast, synoptic fronts, and dry lines,
105 with separation of these different circulations sometimes not possible. In addition, the smoothing and thresholds applied in the object identification methods may result in the exclusion of small scale or weak sea breeze fronts. This is discussed further in Section 3.2.

## 2.2 Offshore wind areas and sea breeze front days

The impact of the sea breeze on wind energy resources is analysed for eight different potential offshore wind areas in southeast-
110 ern and southwestern Australia (Figure 1). These areas are either high priority for offshore wind farm development as declared by the Australian government (Department of Climate Change, Energy, the Environment and Water, 2024), or expected areas for development as part of future energy system planning (Australian Energy Market Operator, 2024). However, there are currently no installed offshore wind farms in Australia.

The areas are described as follows. In southwest Australia, the Bunbury offshore wind area is considered and split into two,
115 referred to here as "Bunbury Nearshore" and "Bunbury Offshore" according to the relative distance from the coast (Figure 1a). In southeast Australia, there are six offshore areas (Figure 1b), including two off the subtropical east coast near the city of Sydney in the state of New South Wales (Newcastle and Illawarra). There are two areas in the Bass Strait between mainland Australia and the island of Tasmania to the south (Gippsland and Tasmania), and two to the west off the coast of the states of Victoria (Southern Ocean) and South Australia (South Australia).

120 For each offshore wind area, a sea breeze front day (SBF day) is defined by the occurrence of a sea breeze object over the adjacent coastal land area, between 10:00 and 21:00 Australian Eastern Standard Time (AEST, UTC + 10) for areas in southeast Australia, and between 10:00 and 21:00 Australian Western Standard Time (AWST, UTC + 8) for areas in southwest Australia. These time zones (AEST and AWST) will sometimes be collectively referred to here as "local standard time" for convenience. Coastal land areas for defining SBF days were subjectively chosen, intended to represent regions where the sea
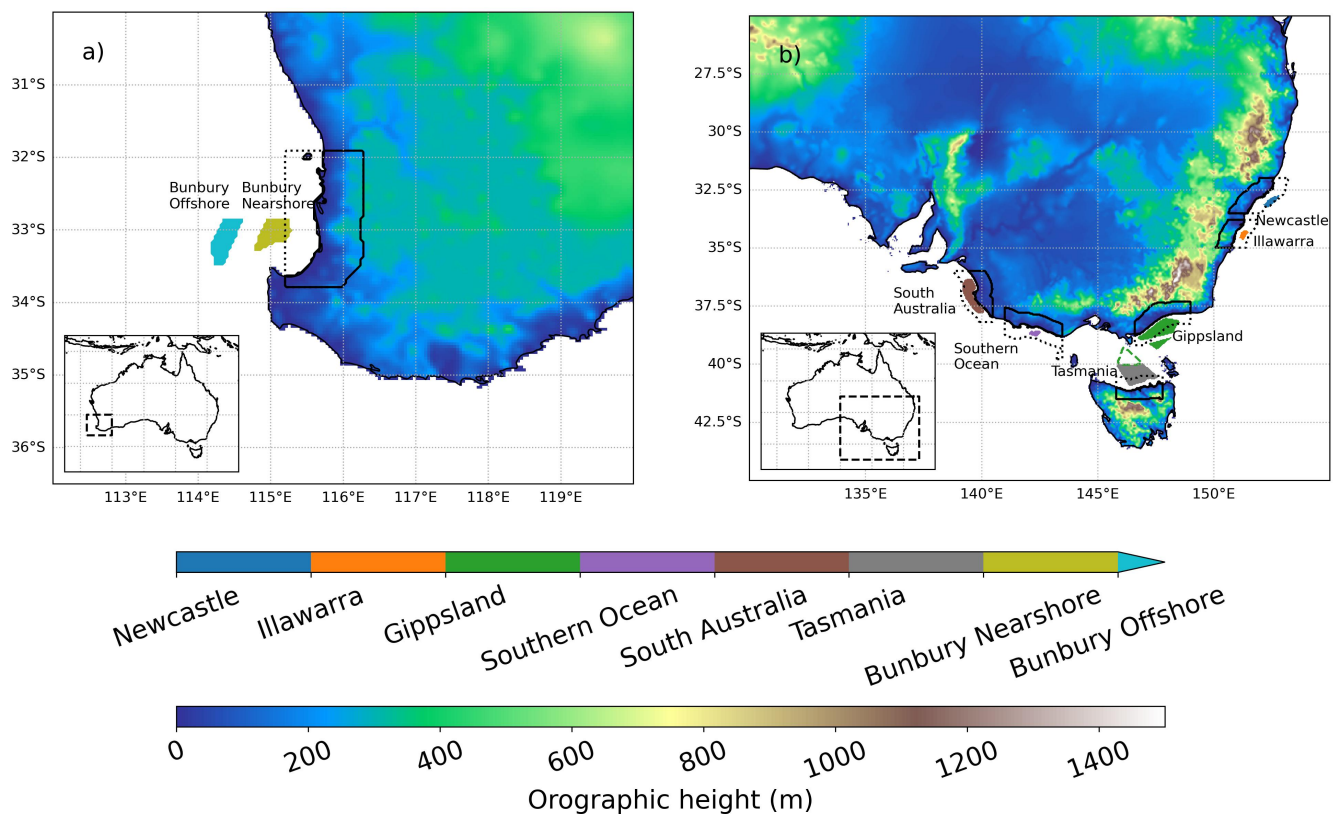
**Figure 1.** Map of offshore wind areas and adjacent coastal land areas in (a) southwestern Australia and (b) southeastern Australia. Each of the eight offshore wind areas are shown with a different colour, and are labelled. The seven adjacent coastal areas over the land, used to define sea breeze front days, are shown with solid black contours. Coastal areas over the sea are shown with a dotted black line, used in the definition of land-sea temperature contrast. Both the onshore and offshore coastal zones extend to a maximum of 50 km inland and offshore, respectively. For the Gippsland offshore wind region (green contours), the official region declared by the Australian government includes a portion in the middle of Bass Strait (dotted green region). However, this portion is removed from analysis here, due to the lack of a clear adjacent coastline for defining sea breeze front days. Topographic data from BARRA-C2 is shown with shading.

125 breeze could potentially influence surface winds within the offshore wind areas, with each area shown in Figure 1. Despite sea breeze objects being mainly identified over the land (see object occurrence maps in Section 3.1), surface winds over adjacent oceans can be influenced due to the broader circulation (Rafiq et al., 2020; Finocchio et al., 2025). The coastal land areas were restricted spatially, such that the extent of each area is within 50 km of the coastline. This limits the potential impacts of steep topography near some of the coastal land areas on sea breeze identification (Figure 1b), where the influence of up-slope

130 mountain breezes can become confounded with the sea breeze. Although there are eight offshore wind areas as described previously, there are only seven unique coastal land areas, due to the two Bunbury areas having the same adjacent coastline (Figure 1a). For the Gippsland offshore wind area, situated off the coast of the state of Victoria, part of the official declared area near the middle of the Bass Strait (see green dotted contour line in Figure 1b) has been ignored in subsequent analysis, due to the lack of a clear adjacent coastline for defining sea breeze front days.

135 In the Results section, the seasonal cycle of SBF days for the different coastal areas are reported, as well as the average wind energy capacity factor on SBF days for each offshore wind area compared with "other days". These other days are defined as days without a sea breeze object identified in each coastal land area. These days may include other diurnally-varying wind processes that could resemble sea breezes, such as the daytime vertical mixing of winds from aloft or up-slope mountain breezes. In addition, these other days could include weak coastal circulations that do not form a sea breeze front of sufficient

140 strength to be identified by our methods.

## 2.3 Land-sea temperature difference

To help explain variability in sea breeze front days in each coastal region, we calculate the land-sea temperature difference ($T_{land} - T_{sea}$) as a measure of sea breeze forcing. For the land temperature, $T_{land}$, we consider hourly near-surface air temperature from BARRA-C2 averaged over the coastal land areas in Figure 1. For the sea temperature, $T_{sea}$, we consider hourly

145 BARRA-C2 near-surface air temperatures averaged over the coastal ocean areas adjacent to each coastal land area, shown by the black dotted lines in Figure 1. The coastal land and ocean areas for calculating $T_{land}$ and $T_{sea}$ are restricted to be within 50 km of the coastline. Hourly $T_{land} - T_{sea}$ values for each area are then resampled to a daily time series, by taking the maximum for each day in local standard time. The monthly mean daily maximum $T_{land} - T_{sea}$ is presented in the Results section.

Although this approach provides a broad measure of sea breeze forcing, there are uncertainties around defining the land-sea

150 temperature difference, with various approaches adopted by previous studies. This includes regionally averaging temperatures in the cross-shore and/or along-shore directions (Cafaro et al., 2019; Xia et al., 2022; Huang et al., 2025), using single model grid values at fixed distances (Bergemann et al., 2017; Arrillaga et al., 2020), and using observed point values at fixed distances in the onshore and offshore directions, such as 300 m, 20 km, or 30 km (Borne et al., 1998; Frysinger et al., 2003; Azorin-Molina et al., 2011), as well as directly on the shoreline (Assireu et al., 2024). Threshold values of $T_{land} - T_{sea}$ are often used

155 as a condition for sea breeze development, but there is a lack of consensus on this threshold, with values such as 0, 1.5 and 3 °C used in the literature (Borne et al., 1998; Azorin-Molina et al., 2011; Xia et al., 2022). In the current study, a regional average is used considering model grid points within 50 km of the coastline, rather than individual points. This is intended to capture the broad mesoscale sea breeze forcing, ignoring small-scale surface temperature variability. This is acknowledged as a potential

uncertainty, with small-scale temperature gradients shown previously to impact sea breeze characteristics (for example, Wang
160   et al., 2017).

## 2.4   Wind power model and energy demand data

Wind energy resources are quantified using capacity factors calculated from hourly BARRA-C2 wind speeds at 100 m above the
surface. This is done over the same 1979–2024 period as for the sea breeze objects. The BARRA-C2 wind speeds are calculated
from $u$ and $v$ wind components, which have been logarithmically interpolated to 100 m height from the original BARRA-C2
165   model-level data. Capacity factors are based on the International Energy Agency (IEA) offshore 10 MW reference wind turbine
(Bortolotti et al., 2019), with a cut-in wind speed of 3 m/s, cut-out wind speed of 25 m/s, and rated power reached at 11 m/s.
The power curve data for the IEA reference turbine is provided by the National Renewable Energy Laboratory at intervals
ranging from 0.5 to 1.0 m/s (Duffy, 2020), with a cubic spline interpolation used to map BARRA-C2 wind speeds onto the
curve (Virtanen et al., 2020). Further details on the IEA reference turbine can be found at https://nrel.github.io/turbine-models/
170   IEA_10MW_198_RWT.html (last accessed 11 November, 2025). Capacity factors are presented for different times of the day,
separately for sea breeze front days and other days, both as spatial maps and spatial averages over each offshore wind area.
Capacity factors will be shown for the Austral summer period (December–February), when sea breezes are more likely to occur
due to relatively intense daytime heating of the land.

It should be kept in mind that there are uncertainties in estimating wind energy potential from the BARRA-C2 reanalysis.
175   Although the regional version of BARRA (BARRA-R2) has demonstrated improvements over other reanalysis models in
simulating wind speeds at turbine hub height (Cowin et al., 2023; Palmer et al., 2025), BARRA-C2 has not yet been thoroughly
evaluated. In addition, there are significant limitations in using wind speeds from gridded models for representing wind energy
at the turbine scale (Davidson and Millstein, 2022). Therefore, the capacity factors reported here should mostly be interpreted
in terms of the relative contribution from sea breezes, with potential biases in the absolute values reported.

180   To help assess the potential value of offshore wind energy resources related to sea breezes, the average daily cycle in re-
gional energy demand is compared with capacity factors for each offshore area on sea breeze front days and other days. Energy
demand data for the eastern regions are obtained from the Australian Energy Market Operator (AEMO) via the NEMOSIS
software package (Gorman et al., 2018). The data are provided regionally for each Australian state in the National Energy
Market (NEM). The capacity factor for each offshore wind region is compared with demand data for the Australian state in
185   closest proximity. The NEM demand data are provided at intervals of 5 minutes, and are subset to hourly intervals corre-
sponding to the BARRA-C2 data. Demand data for the Australian state of Western Australia (including the Bunbury areas) are
obtained directly from AEMO at 30-minute intervals, and are similarly subset to hourly intervals (https://www.aemo.com.au/
energy-systems/electricity/wholesale-electricity-market-wem/data-wem/market-data-wa, last accessed 11 November 2025).
Following Richardson et al. (2025), each energy demand dataset is restricted to the period of 2010–2019 to remove potential
190   impacts of the COVID-19 pandemic from 2020 onwards. As for the capacity factors discussed above, diurnal energy demand
profiles are considered for the Austral summer (December–February).

## 3 Results

### 3.1 Spatial and seasonal variations in sea breeze occurrences

The spatial distribution of sea breeze object occurrence frequency is shown seasonally for southeastern Australia in Figure 2,
and for southwestern Australia in Figure 3, in terms of the average number of days with an object identified. Sea breeze objects
are identified most frequently near the coastline over the land, due to the characterisation of the sea breeze as a front (Section
2.1). The diurnal inland movement of the sea breeze front can be seen through the gradient in object occurrence frequency,
particularly in relatively flat regions such as the western part of eastern Australia (Figure 2), or in southwestern Australia
(Figure 3). In these regions, objects can be seen as far as 300 km inland on average, as defined by an occurrence frequency
contour of 2 days/season. The sea breeze front can propagate further than this (Clarke, 1983), but is not seen here due to the
dissipation of moisture gradients to the point where the strength of the front falls below the selected identification threshold
(see Section 2.1). Although sea breeze objects are identified almost exclusively over the land, the influence of the broader sea
breeze circulation on the boundary layer wind field is expected to extend some distance offshore (for example, Rafiq et al.,
2020; Finocchio et al., 2025).

For coastal regions near significant topography, the locations of the local maxima in sea breeze object occurrence frequency
tend to be shifted away from the coastline and towards the mountains (Figure 2). This can be most clearly seen between the
coastal land regions adjacent to Gippsland and Illawarra (around 36 °S, 149 °E). The sea breeze objects identified there are
likely produced by a combination of coastal and topographic forcing, which are not able to be easily disentangled. This is
consistent with previous idealised modelling studies such as Miao et al. (2003), who have shown that when the sea breeze
occurs simultaneously with differential mountain/valley heating, the front between land and sea air occurs further up-slope.
Inland displacement of detectable sea breeze fronts has also been noted for this region of southeastern Australia by Clarke
(1983).

For both southeastern and southwestern Australia, sea breezes tend to occur most often during the Austral summer (December–
February, Figures 2a and 3a), when differential land-sea surface temperature gradients are largest. The exception appears to
be along the east coast of Australia north of 35°S, where sea breeze objects occur most frequently in the Austral spring
(September–November, Figure 2d). The seasonal cycle is examined in more detail in Figure 4, in terms of sea breeze front
(SBF) days for each of the coastal land areas adjacent to the offshore wind areas. For each region, the maximum in SBF days
occurs some time during the warm season (October–February), with some variations in the peak month between locations. The
maximum monthly SBF day occurrence frequency ranges from around 40% of days in the Southern Ocean area (February)
to 80% of days in the Bunbury area (January). The minimum occurrence frequency ranges from around 20% in the Bunbury
region to nearly 0% in several regions, during June–August.

Figure 4 also shows the mean, daily maximum $T_{land} - T_{sea}$ for each month. The seasonal SBF day cycle generally follows
the same shape as the seasonal cycle in mean $T_{land} - T_{sea}$. However, for some regions, the peak in SBF day frequency occurs
earlier in the year relative to the peak in mean $T_{land} - T_{sea}$. For example, for the Newcastle and Illawarra regions (both on
the east coast), SBF day frequency peaks in October (around 50% of days) even though the monthly mean $T_{land} - T_{sea}$ peaks
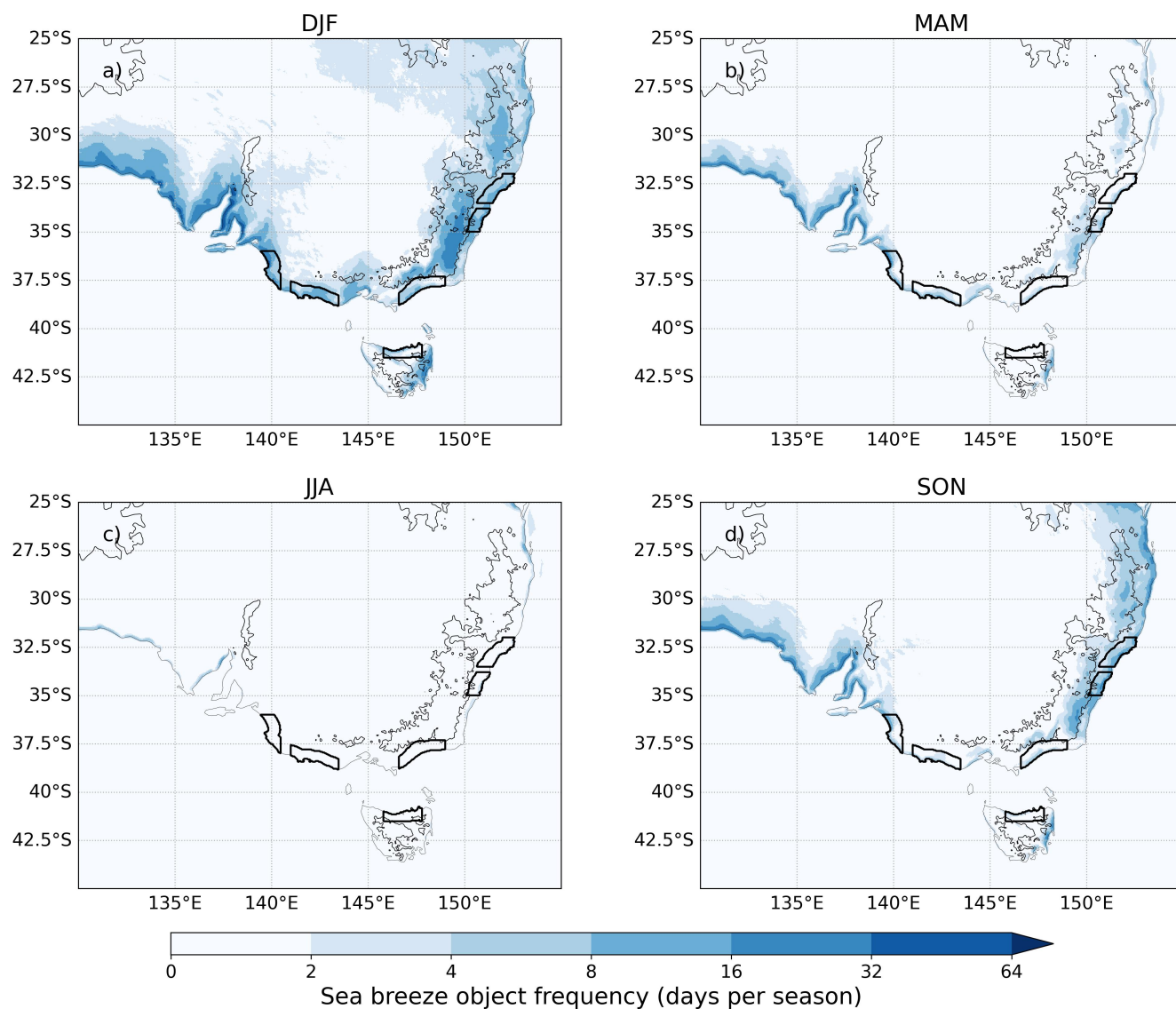
**Figure 2.** The daily frequency of occurrence of a sea breeze object, shown as days per season for (a) December–February (DJF), (b) March–May (MAM), (c) June–August (JJA) and (d) September–November (SON). Shown for southeast Australia using data from 1979–2024. Coastal areas are indicated with a black contour that are adjacent to six declared offshore wind areas (see Figure 1). Note the logarithmic colour scale, intended to highlight inland occurrences of sea breezes. Topography over 500 m used in the BARRA-C2 model is contoured.
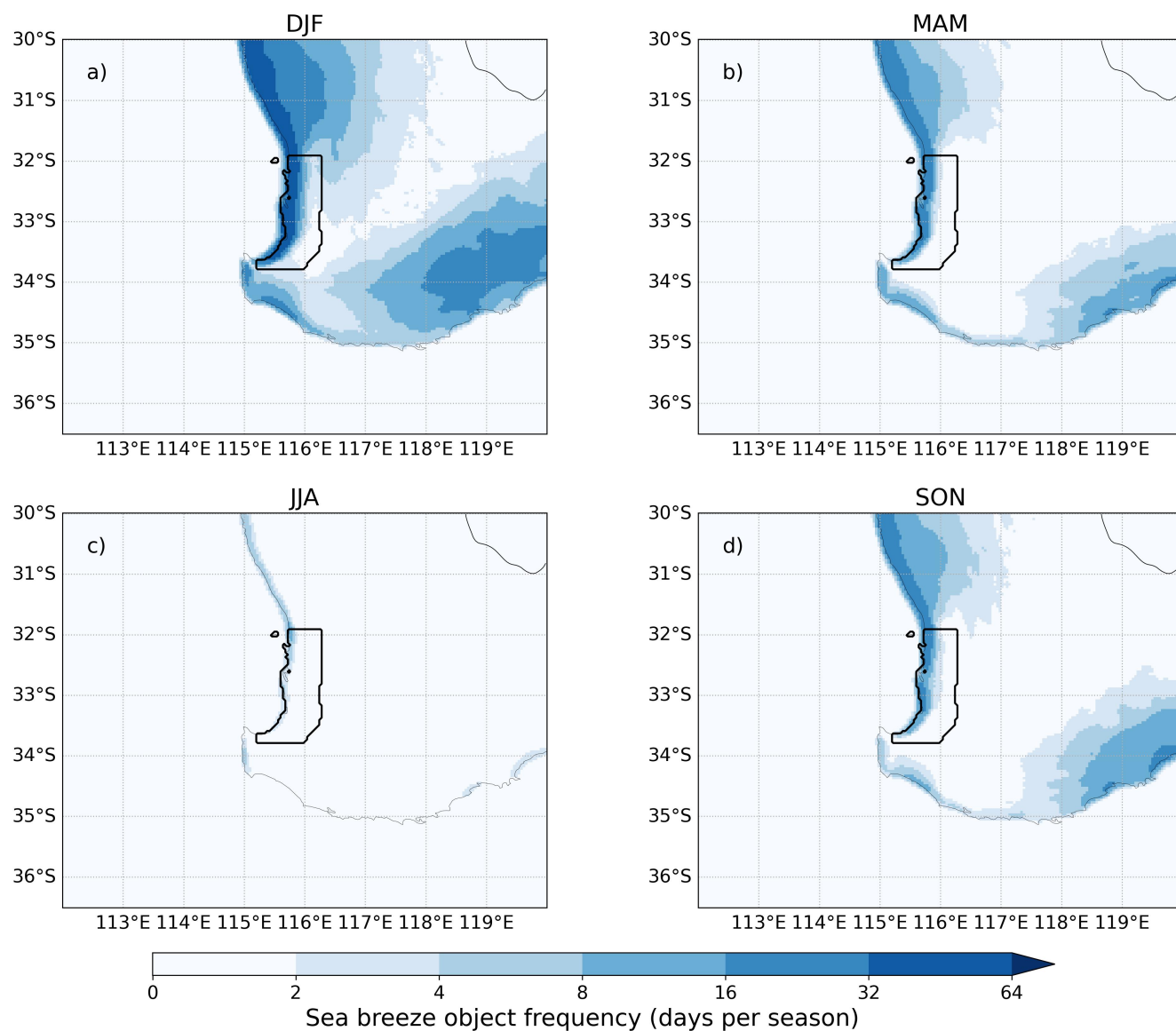
**Figure 3.** As in Figure 2, but for southwestern Australia.
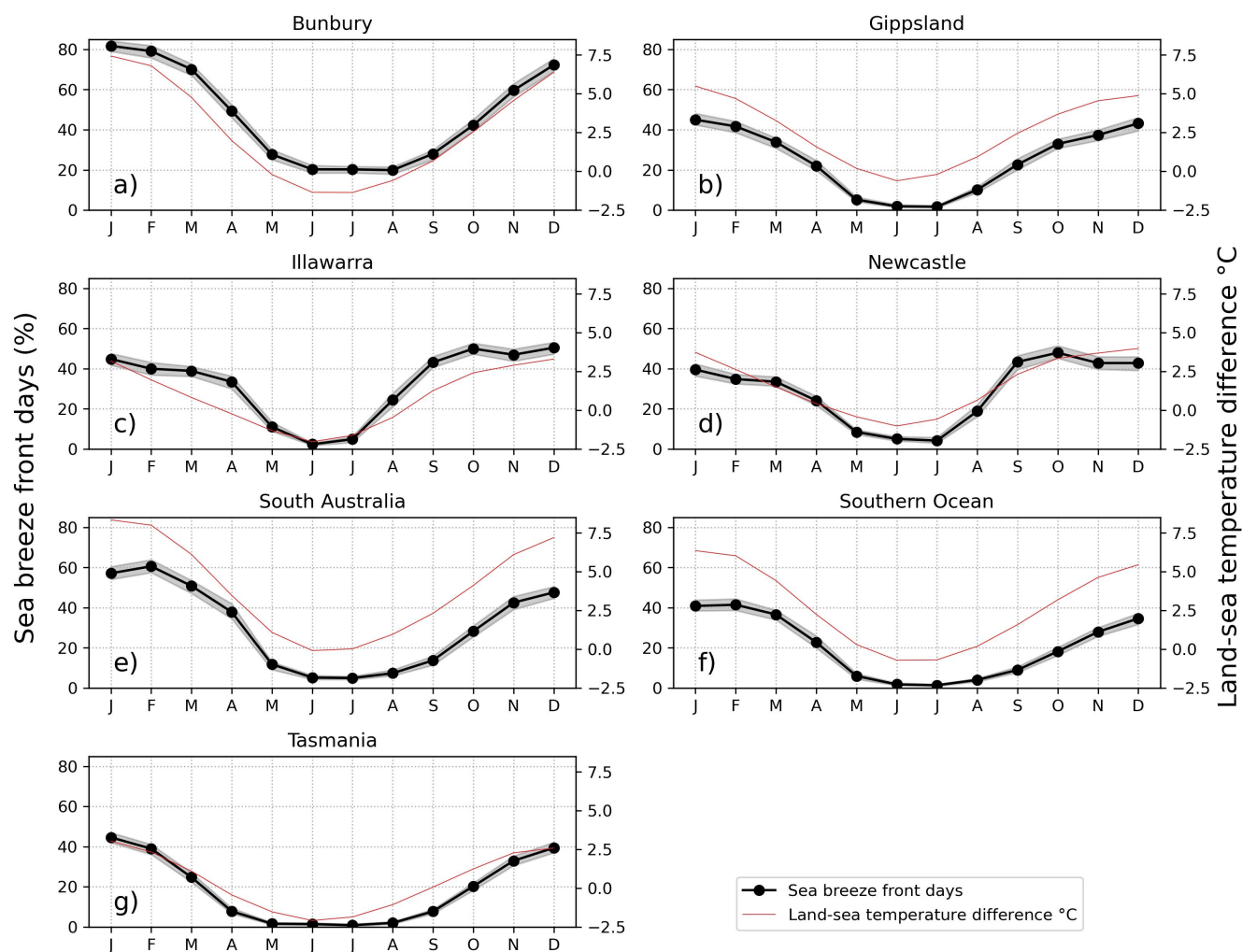
**Figure 4.** (black line) Monthly occurrence frequency of a sea breeze front day for each coastal land area adjacent to the potential offshore wind areas. Shown as a percentage of days. A 90% confidence interval is indicated with grey shading, estimated by randomly re-sampling different years of data, 1,000 times with replacement. The average daily maximum land-sea temperature contrast (°C) is shown for comparison (red lines).

in December–January. This suggests that other factors are influencing the seasonal cycle of SBF days besides the land-sea temperature difference, such as the prevailing wind. Alternatively, the average land/sea temperatures in a broader region may not be an accurate estimate of sea breeze forcing (see Section 2.3). In addition, the variations in SBF day occurrence frequency between regions does not appear to be driven only by differences in the magnitude of $T_{land} - T_{sea}$. For example, Illawarra

230 and Gippsland have approximately the same percentage of SBF days in January (just under 50%), even though the mean $T_{land} - T_{sea}$ varies from around 5 °C (for Gippsland) to around 3 °C (for Illawarra).

### 3.2 Wind resources on sea breeze front days and other days

Figure 5 shows the average diurnal cycle of wind energy capacity factor, averaged over each offshore wind area for SBF days and other days, during the summer (December–February). Capacity factors are compared with the average diurnal cycle

235 of regional energy demand over a 2010–2019 period. The December–February period is analysed here given the relatively high occurrence frequency of an SBF day for most regions (Figure 4), combined with the expectations for hot summertime temperatures leading to increased energy demand (Richardson et al., 2025).

For all regions besides Gippsland and Tasmania, the afternoon wind energy potential is around 15–30% higher on SBF days compared with other days, suggesting that the sea breeze has a positive impact on wind energy resources in those regions

240 during the summer. However, sea breezes may also occur on days with weak prevailing winds, with reduced wind energy potential throughout the morning (for example, the Southern Ocean area, Figure 5e). In addition, there is typically a lull in wind speeds prior to the formation of the sea breeze at around 10:00–12:00 local standard time. As a result, for all regions besides Newcastle, the wind energy potential is reduced on SBF days at some point in the late morning relative to other days. Together, these results demonstrate that although the sea breeze is a source of local wind and typically enhanced wind energy

245 in the afternoon during the summer, it may not always increase wind energy potential, due to its opposition of the existing prevailing wind. For Gippsland and Tasmania, the afternoon wind speed capacity factor is similar, or slightly reduced, on average for SBF days and other days, or slightly reduced on SBF days.

Given the late morning lull and enhanced afternoon winds on SBF days for most regions, the amplitude of the diurnal cycle in capacity factor is generally much larger on those days compared to other days. For example, in the Bunbury Nearshore

250 area (Figure 5g), the average capacity factor on SBF days ranges from 0.43 (at 12:00 AWST) to 0.93 (at 21:00 AWST). In contrast, on other days, there is a reduced (but still significant) diurnal variation in capacity factor over that area (from 0.52 at 10:00 AWST to 0.75 at 19:00). These diurnal variations on other days may be due to weak sea breezes that are not detected by the identification methods, or other diurnally-forced processes such as vertical mixing of winds from aloft to the surface with daytime heating.

255 For regions with enhanced wind energy potential on SBF days, the late afternoon/early evening peak generally coincides with the time of peak energy demand (Figure 5b, c, d, e, g, h). This demonstrates the value of wind energy associated with the sea breeze. In addition, Figure 5 indicates that regional demand is generally higher on SBF days compared with other days. This is likely due to higher surface air temperatures over the land on SBF days (Supplementary Material, Section S2), consistent with hotter land surfaces for sea breeze forcing, which in turn increases the demand load from cooling. The exception for this
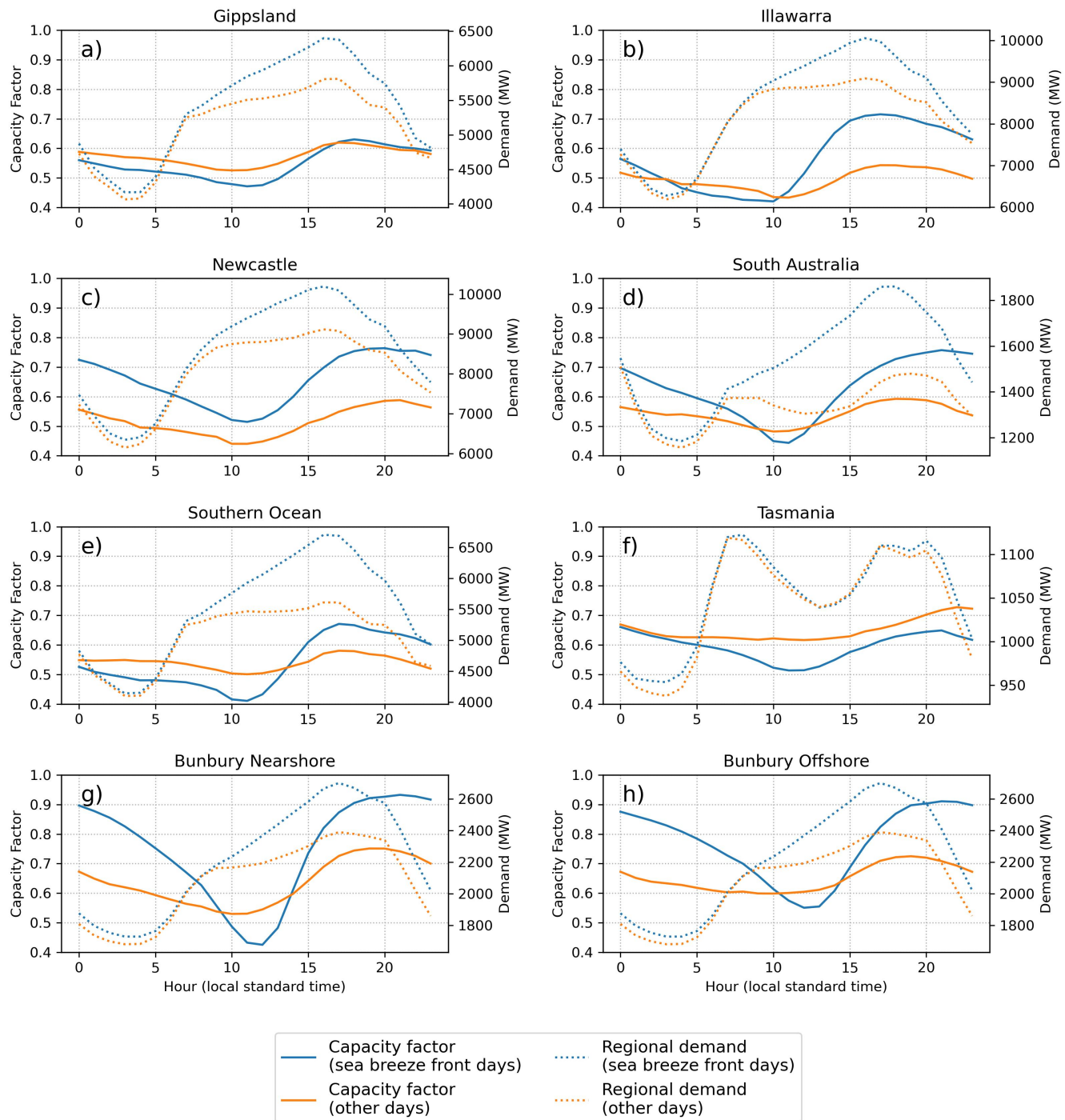
**Figure 5.** Wind energy capacity factor for each hour of the day during December–February, 1979–2024, averaged over each offshore wind area, shown separately for (blue line) sea breeze front days and (orange line) other days. The average regional energy demand for each hour of the day, using data from 2010–2019, is shown with dotted lines for comparison.

260 relationship is the region of Tasmania, where it has been shown previously that energy demand does not increase with hotter maximum temperatures (Richardson et al., 2025).

Figure 6 shows the average wind direction throughout the day on SBF days and other days. The average wind field on SBF days consists of several different types of sea breezes, associated with the direction of the prevailing background winds in the morning. This includes "pure" sea breeze conditions with predominately offshore winds in the morning (Gippsland and South

265 Australia, Figures 6a, d) and "corkscrew" sea breeze conditions with the land to the right of the prevailing winds (Illawarra, Newcastle, Southern Ocean, Tasmania, Bunbury Nearshore and Offshore, Figures 6b, c, e, f, g and h). In the afternoon, the sea breeze direction may either be mostly onshore, or alongshore. Alongshore flow has been shown by previous studies, including in Brazil (Assireu et al., 2024) and Perth (near the Bunbury area, see Rafiq et al., 2020), due to the interaction of the sea breeze with the synoptic wind direction.

270 On days without a SBF, the prevailing background wind in the morning may already be onshore (for example, in the Gippsland region, see Figure 6a), or be alongshore with the land to the left of the prevailing wind (for example, in the Illawarra region, Figure 6b). In the latter case, the afternoon winds turn onshore, and could represent weak backdoor sea breezes with weak frontal gradients. In the former case with onshore prevailing winds, the wind speeds strengthen during the afternoon. This could be due to sea breeze circulations embedded within the onshore flow that may have weak fronts, potentially too weak

275 to be identified (Reible et al., 1993). Alternatively, the afternoon strengthening of winds could be related to other mechanisms such as the vertical mixing of higher wind speeds to near the surface with daytime heating. However, the potential for weak sea breezes to exist on "other days" should be noted when interpreting results. In summary, sea breezes are interpreted here as coastal circulations leading to strong fronts over the land, with weaker circulations possible on other (non-SBF) days. The results in this section suggest that stronger circulations with fronts over the land are more relevant for wind energy resources

280 (Figure 5).

### 3.3 Co-variability of sea breeze front days across wind energy zones

In Section 3.2, it was demonstrated that sea breeze front (SBF) days and other days have different prevailing winds in the morning (Figure 6), suggesting that the background wind direction has a strong influence on sea breeze formation consistent with previous studies (Arritt, 1993; Steele et al., 2013). It follows that for a given large-scale wind pattern over southeastern

285 or southwestern Australia, there will be coastal regions where sea breeze fronts are more or less likely to be identified, due to prevailing winds being onshore/offshore in different regions, for example. This is demonstrated here for two offshore wind areas with opposite facing coastlines during the December–February period: Illawarra and Southern Ocean (see locations in Figure 1b).

Figure 7a shows that in the early morning (05:00 AEST) on Illawarra SBF days, there is a synoptic pattern with northerly

290 alongshore winds relative to the Illawarra coastline, on average. As discussed in Section 3.2, this is favourable for corkscrew sea breeze formation. At the same time, this synoptic pattern produces onshore prevailing winds for the Southern Ocean area that generally favours non-SBF conditions (Figure 7a). In the afternoon, strong onshore flow develops in the Illawarra region (Figure 7c), whereas in the Southern Ocean region, the onshore winds have only increased in magnitude (consistent with
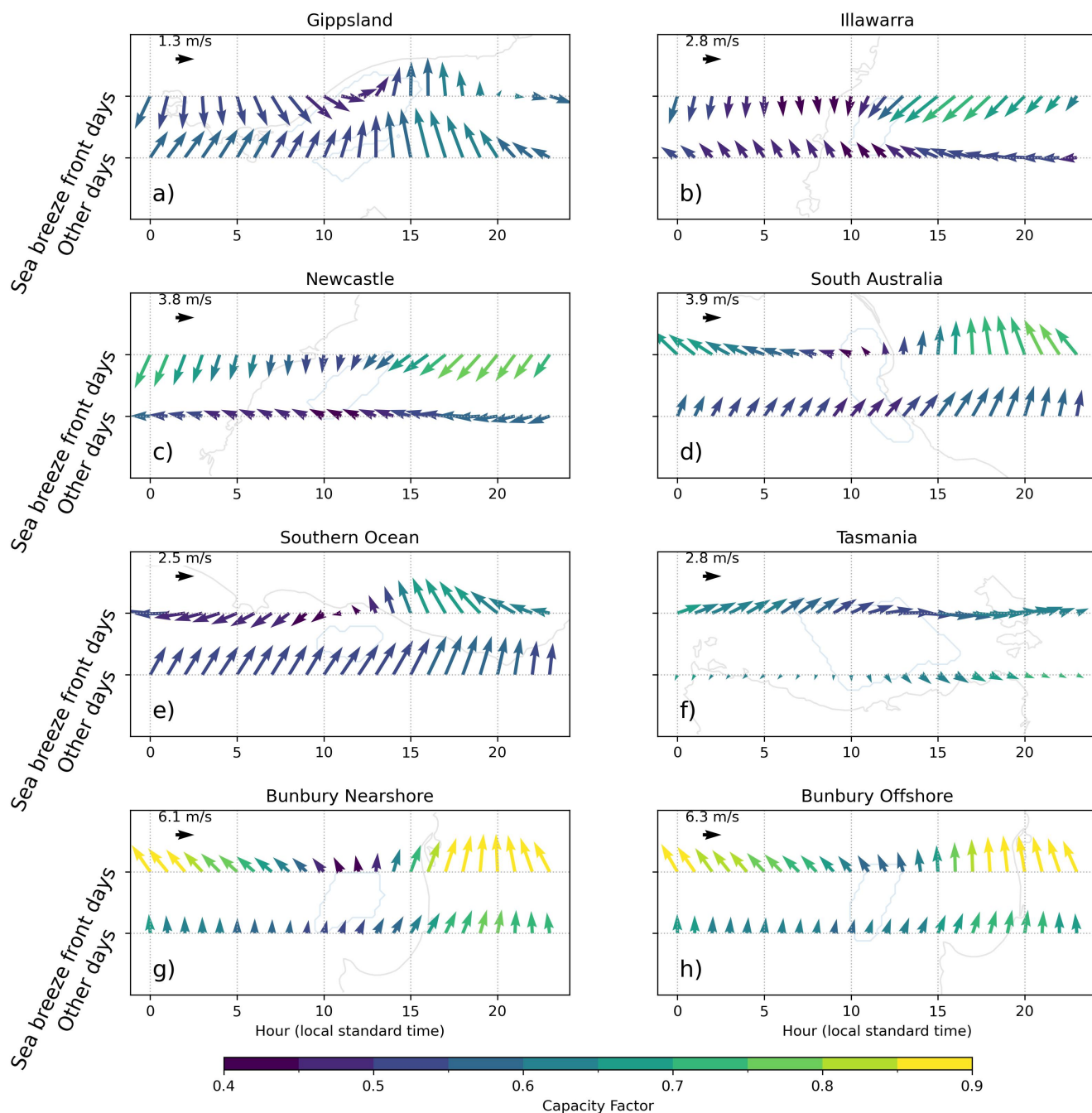
**Figure 6.** Hourly 100 m $u$ and $v$ wind components averaged over each offshore wind area for each hour of the day during December–February, shown as wind vector plots separately for sea breeze front days (upper vectors) and other days (lower vectors). Vectors are coloured by the corresponding average capacity factor. The coastline and offshore wind areas are shown in the background of each panel for reference, in grey and blue contours, respectively.
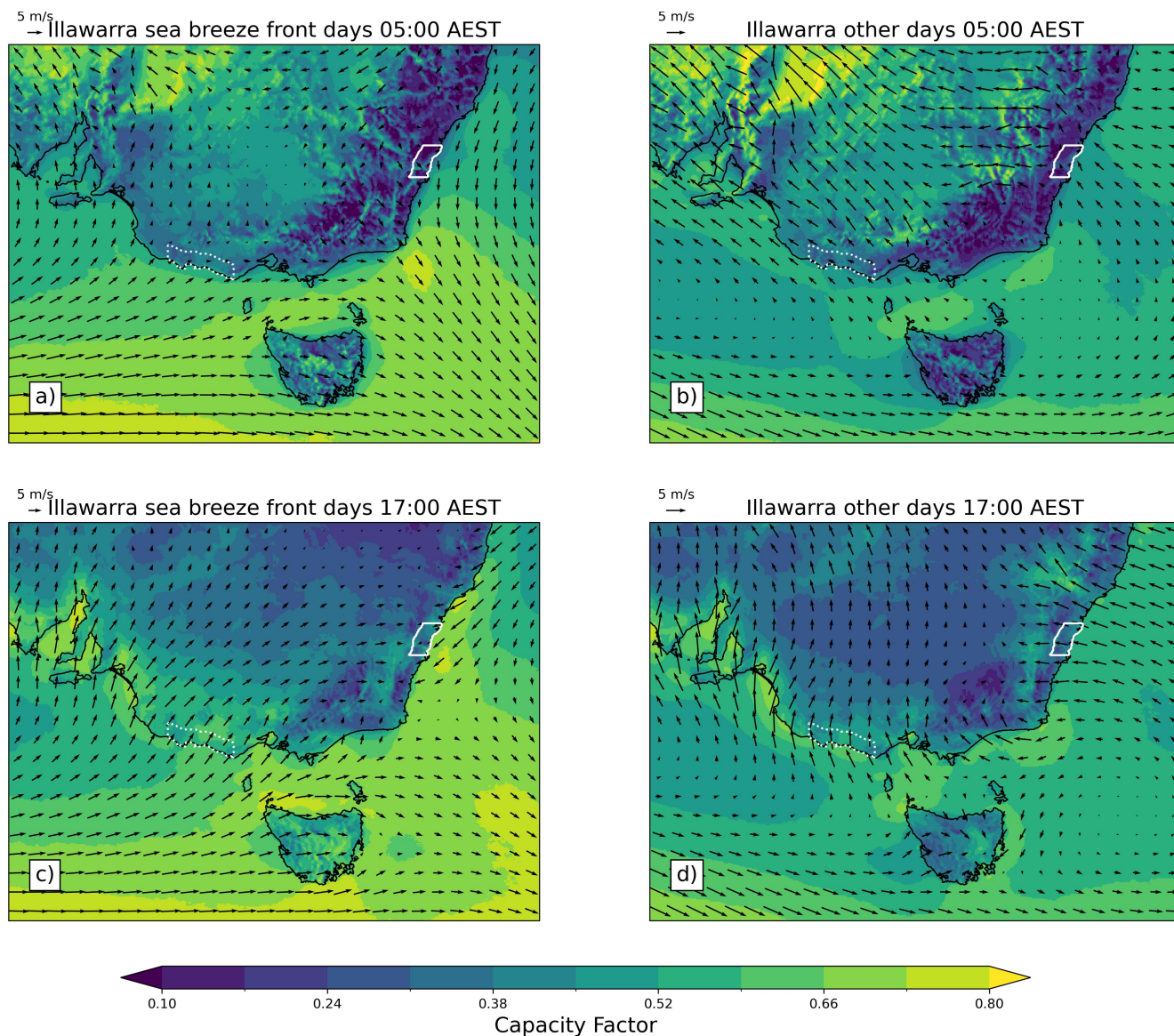
**Figure 7.** Spatial map of 100 m *u* and *v* wind components and capacity factor, averaged over (a, c) sea breeze front days and (b, d) other days for the Illawarra offshore wind area. Averages are calculated during December–February, for (a, b) 05:00 Australian Eastern Standard Time (AEST) and (c, d) 17:00 AEST. The location of onshore coastal areas adjacent to the Illawarra and Southern Ocean offshore wind areas are highlighted with a solid and dotted white contour line, respectively.

the wind direction on other days for the Southern Ocean region in Figure 6e). This suggests sea breeze front formation in
295    the Illawarra region, while for the Southern Ocean region, the afternoon winds may have strengthened due to weak coastal
circulations embedded within the prevailing flow, or due to vertical mixing of higher wind speeds from aloft.

Conversely, on days without a SBF in the Illawarra region, there is onshore flow there in the morning (Figure 7b), with alongshore flow relative to the Southern Ocean coastline with land to the right, favourable for corkscrew sea breeze formation. In the afternoon, the opposite pattern can be seen compared with SBF days in the Illawarra region: strong onshore flow has
300   developed in the Southern Ocean region, whereas in the Illawarra region, the onshore winds have only increased in magnitude (Figure 7d). For completeness, Figure 8 shows the same analysis but for Southern Ocean SBF days and other days. The figure essentially demonstrates the inverse pattern, whereby the Southern Ocean SBF days occur with offshore flow in the morning, with unfavourable SBF conditions for the opposite-facing Illawarra coastline.

Figure 9 extends this analysis, showing anomaly maps of sea breeze objects identified on SBF days for each offshore
305   wind area during December–February. This figure demonstrates that when sea breezes are identified on east-facing coastlines (Illawarra, Newcastle, or Gippsland), they are less likely to be identified on west-facing coastlines (including South Australia or Southern Ocean) due to the orientation of the prevailing winds, similar to the example shown previously for the Illawarra and Southern Ocean regions. The opposite is true when sea breeze fronts are identified on the west-facing coastlines (that is, negative anomalies are seen over the east-facing coastlines on those days), and the same effect can be seen for north/south
310   facing coastlines (Tasmania and Southern Ocean, Figure 9f) and the adjacent coastlines in southwestern Australia (Figure 9g). The correlation of SBF day occurrences between each region in southeast Australia is quantified further in the Supplementary Material using the Odds Ratio (Section S3). That analysis shows, for example, that the odds of a SBF day occurring in the Illawarra or Southern Ocean regions is approximately halved when a SBF day occurs in the other region. In contrast, the odds of a SBF day occurring in Illawarra or Gippsland is 2.7 times higher when there is a SBF day in the other region.

315   Finally, this behaviour is related to late-afternoon available wind energy (18:00 local standard time) by showing spatial maps of the difference in capacity factor between regional SBF days and other days (Figure 10). The 18:00 local standard time difference is approximately the time of peak energy demand and sea breeze wind speeds (Figure 5). For the regions of Illawarra, Newcastle and Gippsland, there is generally more local available offshore wind energy on SBF days along the east coast (up to a 0.1–0.2 increase in capacity factor, Figure 10a–c). There is similar or reduced available offshore wind energy
320   along the South Australia and Southern Ocean regions (up to a 0.1 reduction), likely due to a reduction in sea breeze activity as described previously (Figure 9). In addition, there are localised reductions in available wind energy in the inland regions adjacent to each of the coastal regions where SBFs are identified (by as much as 0.2–0.3 in capacity factor), but with a general increase in available wind energy across large parts of inland southern Australia, likely due to enhanced synoptic-scale wind speeds.

325   In contrast, on SBF days over the west-facing coastal locations of South Australia and Southern Ocean, there are decreases in local offshore wind energy availability over large sections of the east coast (up to around 0.1 in capacity factor), as well as along the northern coast of Tasmania (Figure 10d–e), with local increases in available wind energy for the offshore regions of South Australia and the Southern Ocean. Again, this is likely due to the behaviour of sea breeze activity described previously in this section. There tends to be widespread decreases in available wind energy throughout inland parts of southern Australia
330   on these SBF days, potentially due to reductions in onshore synoptic-scale wind speeds. For SBF days in Tasmania (Figure 10f), there are small local offshore increases in available wind energy due to sea breeze activity, but large decreases in offshore
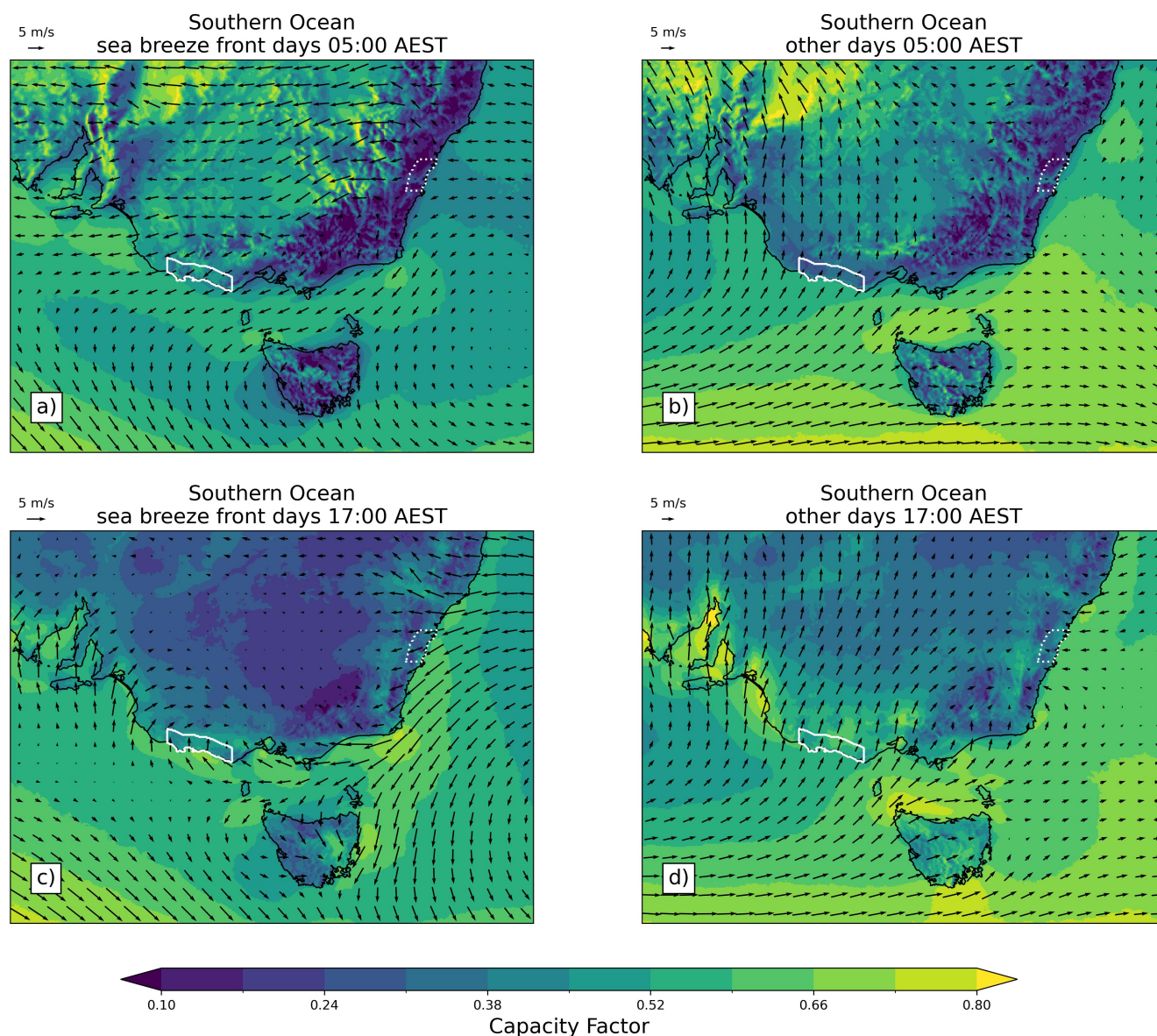
**Figure 8.** As in Figure 7, but on sea breeze front days and other days for the Southern Ocean offshore wind area. The location of onshore coastal areas adjacent to the Southern Ocean and Illawarra offshore wind areas are highlighted with a solid and dotted white contour line, respectively.
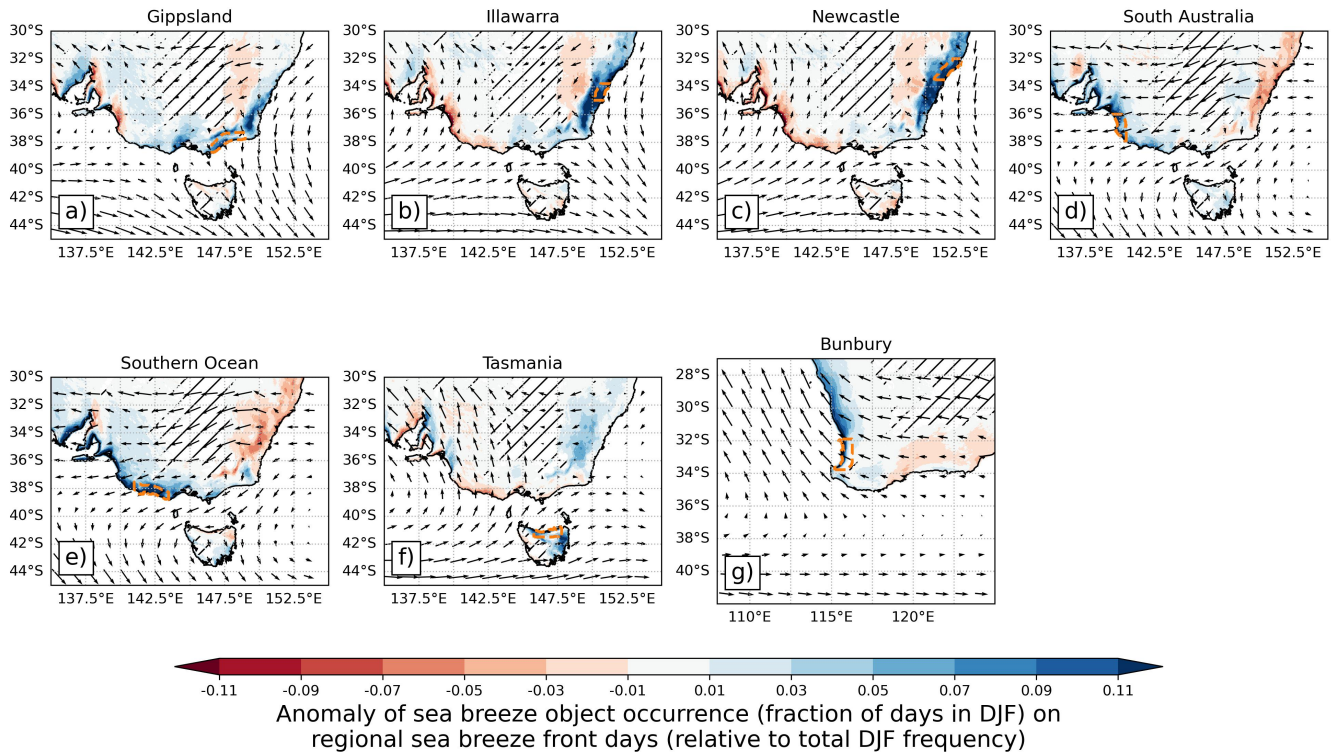
**Figure 9.** Map of sea breeze object occurrence frequency anomaly (fraction of days) between regional sea breeze front (SBF) days and total days, for December–February. Positive values for a given region represent a greater frequency of sea breeze object occurrences, compared with the frequency on all days. In each panel, the average $u$ and $v$ wind components over all SBF days for that region at 05:00 local standard time are shown with vectors, as an estimate of the prevailing background wind. The coastal area that is used to define regional SBF days is highlighted with an orange contour line. Hatching represents areas with a total daily sea breeze occurrence frequency less than 1.5% (equivalent to 1.35 days per December–February period, see maps in Figures 2a and 3a), where data has been removed from the plot, for clarity.

regions to the south of mainland Australia (up to a 0.2 reduction in capacity factor). This is likely associated with reductions in synoptic wind speeds, with decreases also in the Gippsland offshore region potentially due to reduced sea breeze activity. On Bunbury SBF days (Figure 10g), there are significant increases in local offshore wind availability near the Bunbury region, and significant decreases inland as well as offshore to the south of the continent.
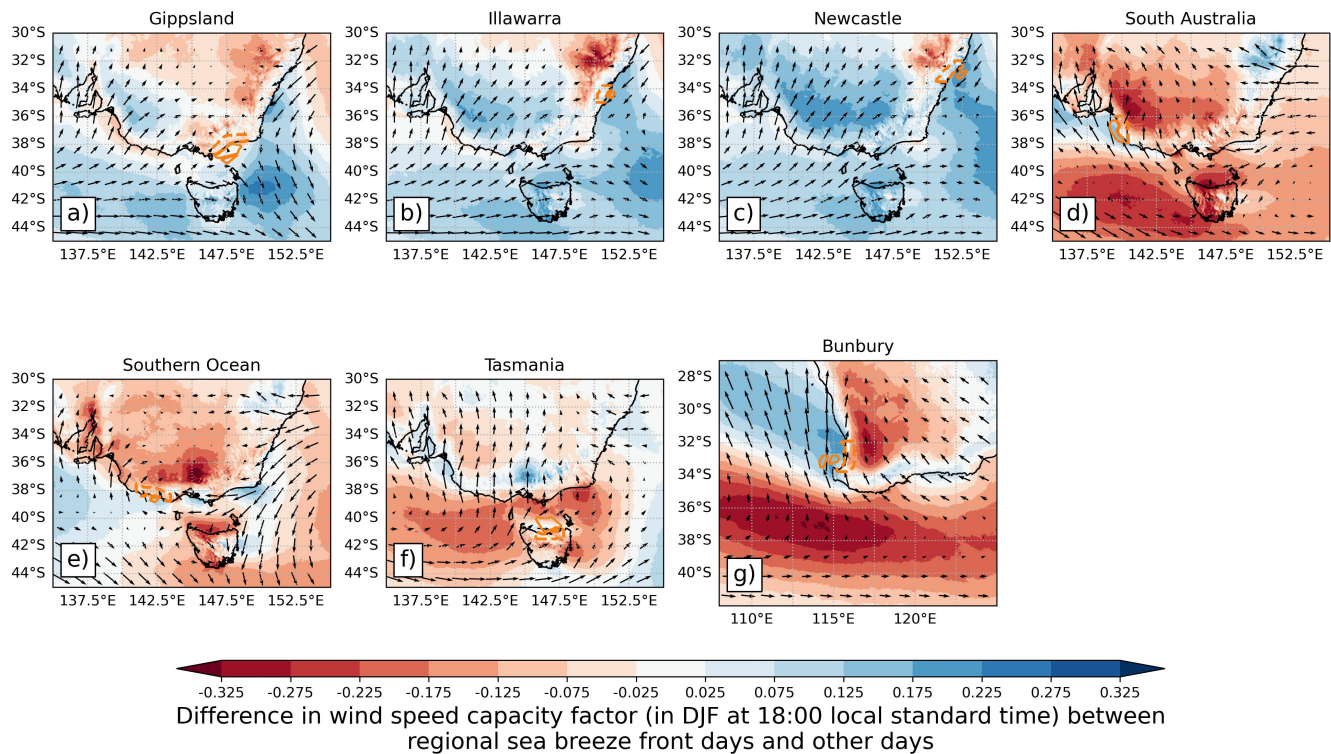
**Figure 10.** Map of the difference in wind energy capacity factor between regional sea breeze front (SBF) days and other days at 18:00 local standard time during December–February. Positive values represent higher capacity factors on SBF days compared with other days. Each panel shows the difference in capacity factor for a different region, with the region used to define SBF days shown in a dashed orange contour. The location of the adjacent offshore wind areas are also shown in orange contours. Average 100 m wind vectors on SBF days are shown at 18:00 local standard time.

## 4 Discussion

A new method for identifying sea breezes as frontal objects (Brown et al., 2025b) has been applied to a km-scale atmospheric reanalysis dataset over Australia, for the period 1979–2024. This method has enabled a robust assessment of sea breeze occurrences for the first time across multiple coastlines in this region, using a single, physically-based diagnostic approach. The spatial and seasonal distribution of sea breeze occurrences are analysed over southeastern and southwestern Australia, with a focus on key potential offshore wind areas.

Maps of sea breeze object occurrence frequency indicate that sea breeze objects are most often identified over coastal land regions during the Austral summer and spring (September–February), with some variations between regions (Figures 2–4). For example, in southern regions such as Gippsland, the peak in the proportion of days with a sea breeze object is in December–January (45% of days, see Figure 4b), whereas for more northern regions such as Newcastle, the peak is in October (50% of days, see Figure 4d). This latter maximum during the Austral spring is similar to findings for the relatively northern region of southeast Queensland by Soderholm et al. (2017), while the maximum in summer for the southern regions is similar to other studies near the Bunbury and South Australia regions (Masselink and Pattiaratchi, 2001; Pazandeh Masouleh et al., 2016). Details on the seasonal cycle in sea breeze occurrences for these previous studies can be found in the Supplementary Material (Section S1).

The seasonal cycle of sea breeze occurrences broadly appears to follow the monthly mean, daily maximum land-sea temperature difference ($T_{land} - T_{sea}$). The mean $T_{land} - T_{sea}$ is representative of sea breeze forcing, and peaks during the warm season due to daytime heating over the land. However, $T_{land} - T_{sea}$ cannot explain some details of the seasonal cycle and variations between regions. For example, as discussed previously, Newcastle sea breeze occurrences peak in October, whereas $T_{land} - T_{sea}$ is maximised in December–January (Figure 4d). Although other factors such as the prevailing wind direction may influence the variability in sea breeze occurrences (Arritt, 1993), it is also possible that $T_{land} - T_{sea}$ as defined here is not an accurate measure of sea breeze forcing. As discussed in Section 2.3, there does not appear to be consensus amongst previous studies on how to define $T_{land} - T_{sea}$. Future work could investigate the spatial and temporal scales of land and ocean temperatures that are relevant for forcing the sea breeze.

During the Austral summer (December–February), sea breezes generally provide enhanced wind energy potential in the offshore wind areas examined during the afternoon on average, relative to other days without sea breeze fronts identified. This was observed for six out of the eight offshore wind areas in southeastern and southwestern Australia (all regions except Gippsland and Tasmania, see Figure 5). In contrast, for all but one of the offshore wind regions (Newcastle), sea breeze formation was associated with decreased wind energy potential during the morning on average. This could be due to preferential sea breeze formation on days with relatively weak prevailing winds, as well as sea breeze surface winds that oppose the existing prevailing winds. The latter process is consistent with a late-morning minimum in capacity factor for most regions, at around 10:00 to 12:00 local standard time, prior to the onset of the sea breeze (Figure 5). These calm periods prior to sea breeze formation have been previously described as offshore "calm zones" by previous studies (Steele et al., 2015), and have implications for the diurnal cycle of wind energy capacity factor in coastal regions.

370  Sea breezes are shown to typically be identified on days during summer with relatively high regional energy demand on average (Figure 5). This is likely due to the tendency for sea breezes to occur on days with hot surface air temperatures over the land (see Supplementary Material Section S2), providing an enhanced land-sea thermal contrast for sea breeze forcing, while also increasing electricity demand for cooling of residential buildings. Furthermore, wind energy capacity factors on days with a sea breeze identified tend to peak at a similar time to energy demand, meaning that offshore wind could potentially provide

375  a useful source of energy during peak demand periods. This is similar to the findings of Pickering et al. (2020) in the alpine regions of Switzerland, who found that diurnal variability in wind resources tends to peak in the afternoon during the summer, due to topographically-forced local winds. Afternoon peaks in local wind energy resources, including due to the sea breeze, could also offset the diurnal reduction in solar energy production in the late afternoon.

The results in Section 3.2 demonstrate that days with a sea breeze identified and days without a sea breeze have very

380  different prevailing wind direction in the morning for a given region, on average (Figure 6). This is consistent with many previous studies that have shown the prevailing wind to have a strong impact on the occurrence of sea breezes and/or detectable fronts (for example, Arritt, 1993; Reible et al., 1993), and therefore the diurnal cycle of wind energy potential (Steele et al., 2015). For example, onshore winds in the morning were found to occur on days without a sea breeze front, as evidenced by the morning wind direction (for example, in Gippsland, Figure 6a). As a result, for a given synoptic-scale wind (westerlies,

385  for example), there are some coastlines with favourable sea breeze conditions, including offshore prevailing winds (east-facing for westerly prevailing winds), and some with unfavourable conditions including onshore prevailing winds (west-facing for westerly prevailing winds). This can be seen in the sea breeze object dataset, with sea breeze occurrences tending to cluster on east and west-facing coastlines (Figure 9). This is consistent with previous studies that have investigated sea breeze characteristics for sets of idealised opposing coastlines (Steele et al., 2013), but is shown here for all coastlines throughout a

390  regional domain using a dataset of sea breeze objects. The clustering of sea breezes on east and west-facing coastlines can also impact the late-afternoon wind energy availability in different regions (Figure 10), and may therefore have implications for managing afternoon energy demand and supply, assuming that these regions of energy generation could be connected in the same system. Results here suggest that diversifying wind generation to multiple coastlines could provide added energy security on high demand days, particularly during the critical late-afternoon high-demand period.

395  The findings here are based on the separation of days with a sea breeze and days without a sea breeze. This separation is defined using the occurrence of a moisture front over the land associated with the sea breeze circulation. However, there are uncertainties in defining these sets of days. For example, coastal circulations are possible (in theory) whenever there is a gradient in surface temperature along the coastline, but here we only define a sea breeze when there is a front that exceeds a certain threshold (see Section 2.1). Figure 6 suggests that there is some turning and strengthening of the wind on days without

400  an identifiable sea breeze front (for example, in the Illawarra region, Figure 6b). This could represent weak coastal circulations without the formation of a strong sea breeze front, and some of the average "other day" wind profiles in Figure 6 could be classified as backdoor sea breeze conditions following other studies (Miller et al., 2003). There is also potential evidence for circulations embedded in onshore prevailing winds that may not have strong frontal gradients (Reible et al., 1993), based on afternoon increases in onshore winds on some "other day" profiles (Figure 6). In addition, the diurnal variability of the winds

405 on days with a sea breeze object could be produced by several different mechanisms. Aside from the sea breeze, this could also include topographically-forced circulations (up-slope mountain breezes), outflow from convection, or vertical mixing of winds from aloft to the surface, for example. The disentangling of these different processes is important for considering the relative contributions of different local wind processes to energy resources, and could be the focus of additional modelling work in the future. Finally, the results presented here are subject to uncertainties in the representation of sea breezes and associated winds

410 in the reanalysis model dataset (BARRA-C2), with similar models shown previously to have significant errors at certain times of the day (Davidson and Millstein, 2022). Evaluation of these reanalysis datasets using wind data at hub height is a critical avenue of future work for wind resource research.

## 5 Conclusion

We investigated the impact of sea breezes on offshore wind resources in southeastern and southwestern Australia, using a

415 historical dataset of sea breeze objects over the period 1979-2024. Key findings are listed as follows:

- Sea breeze occurrences in southeastern and southwestern Australia generally follow a similar seasonal pattern to the mean, daily maximum land-sea temperature contrast, with both generally peaking during the Austral summer. However, some regions (northeast coastal regions including Newcastle and Illawarra) have a peak in sea breeze occurrences shifted to the austral Spring (September–November), earlier than the maximum in land-sea temperature contrast.

420 - For six out of the eight offshore wind areas examined here, there is around 15–30% more available wind resources on sea breeze front days during the afternoon in the Austral summer, compared with other days. In contrast, there is generally less available wind resources during the morning on sea breeze front days, due to calm periods where the sea breeze flow opposes the existing prevailing wind.

- Sea breezes are generally shown to occur on days with high regional energy demand, with an afternoon peak in wind

425 energy that broadly aligns with the afternoon peak in demand. Therefore, wind energy associated with the sea breeze is potentially valuable for balancing energy demand during afternoon peak periods in the summer.

- When sea breezes occur on east-facing coastlines, they are less likely to occur on west-facing coastlines (and vice-versa), due to the role of the prevailing winds in providing favourable conditions for formation. This has implications for correlation of afternoon wind resources between regions

430 These results could help guide strategic decisions on offshore wind farm development and energy system planning, with the goal of providing reliable energy supply in the Australian network. For example, results here suggest that offshore wind energy placed along a range of diverse coastal areas could help with balancing demand in the Australian energy market during the afternoon, especially on hot, high demand days. More broadly, we have highlighted the importance of sub-daily local wind variations (in this case, the sea breeze along the coast) for providing wind energy resources, and therefore the need for

435 sufficiently high resolution data to capture these variations in resource assessments (such as a km-scale reanalysis, as in this

case). In addition to sea breezes, local wind variations can be associated with topographic flows or low-level nocturnal jets, for example. These local wind variations should be considered when assessing potential wind farm sites or the performance of energy systems with large amounts of wind energy. Future work should continue to assess the impact of local wind processes, including sea breezes, on wind energy resources, both onshore and offshore.

440 *Code and data availability.* A daily dataset of sea breeze objects, derived from BARRA-C2 over Australia for the 1979–2024 period, is available at https://doi.org/10.5281/zenodo.18012825 (Brown and Vincent, 2025). Software for producing the sea breeze object dataset is available in Brown et al. (2025a), while software for analysis and figures presented here is available at: https://doi.org/10.5281/zenodo. 18012631. BARRA2 data is made available through the Australian National Computational Infrastructure, NCI (https://dx.doi.org/10.25914/ 1x6g-2v48). Energy demand data and offshore wind area shapefiles are available through the Australian Energy Market Operator (https: 445 //www.aemo.com.au) and the Australian Government Department of Climate Change, Energy, the Environment and Water (https://www. dcceew.gov.au/energy/renewable/offshore-wind/areas). Power curve data for the International Energy Agency 10 MW offshore reference wind turbine is available through the National Renewable Energy Laboratory https://nrel.github.io/turbine-models/IEA_10MW_198_RWT. html.

*Author contributions.* AB and CV conceptualized the research and designed the methods. AB performed the formal analysis and visualiza-450 tion. AB and CV contributed to writing.

*Competing interests.* The authors declare that they have no conflict of interest.

*Acknowledgements.* This research was supported by the Australian Research Council Centre of Excellence for the Weather of the 21st Century (CE230100012), with the assistance of resources from the National Computational Infrastructure (NCI), an NCRIS enabled capability supported by the Australian Government. We acknowledge the contribution of Rachael Isphording, who providing renewable energy zone 455 masks, as well as Doug Richardson who provided useful information and advice on energy demand data.

# References

Arrillaga, J. A., Jiménez, P., Vilà-Guerau de Arellano, J., Jiménez, M. A., Román-Cascón, C., Sastre, M., and Yagüe, C.: Analyzing the Synoptic-, Meso- and Local- Scale Involved in Sea Breeze Formation and Frontal Characteristics, Journal of Geophysical Research: Atmospheres, 125, https://doi.org/10.1029/2019JD031302, 2020.

460 Arritt, R. W.: Numerical modelling of the offshore extent of sea breezes, Quarterly Journal of the Royal Meteorological Society, 115, 547–570, https://doi.org/10.1002/qj.49711548707, 1989.

Arritt, R. W.: Effects of the Large-Scale Flow on Characteristic Features of the Sea Breeze, Journal of Applied Meteorology and Climatology, 32, 116–125, https://doi.org/https://doi.org/10.1175/1520-0450(1993)032<0116:EOTLSF>2.0.CO;2, 1993.

Assireu, A. T., Fisch, G., Carvalho, V. S., Pimenta, F. M., de Freitas, R. M., Saavedra, O. R., Neto, F. L., Júnior, A. R., Oliveira, D. Q., Lopes,

465 D. C., de Lima, S. L., Marcondes, L. G., and Rodrigues, W. K.: Sea breeze-driven effects on wind down-ramps: Their implications for wind farms along the north-east coast of Brazil, Energy, 294, https://doi.org/10.1016/j.energy.2024.130804, 2024.

Australian Energy Market Operator: Appendix 3. Renewable Energy Zones. Appendix to the 2024 Integrated System Plan for the National Energy Market, https://www.aemo.com.au/energy-systems/major-publications/integrated-system-plan-isp/2024-integrated-system-plan-isp, accessed: 10 November, 2025, 2024.

470 Azorin-Molina, C., Chen, D., Tijm, S., and Baldi, M.: A multi-year study of sea breezes in a Mediterranean coastal site: Alicante (Spain), International Journal of Climatology, 31, 468–486, https://doi.org/10.1002/joc.2064, 2011.

Bao, S., Pietrafesa, L., Gayes, P., Noble, S., Viner, B., Qian, J. H., Werth, D., Mitchell, G., and Burdette, S.: Mapping the Spatial Footprint of Sea Breeze Winds in the Southeastern United States, Journal of Geophysical Research: Atmospheres, 128, https://doi.org/10.1029/2022JD037524, 2023.

475 Bergemann, M., Khouider, B., and Jakob, C.: Coastal Tropical Convection in a Stochastic Modeling Framework, Journal of Advances in Modeling Earth Systems, 9, 2561–2582, https://doi.org/10.1002/2017MS001048, 2017.

Borne, K., Chen, D., and Nunez, M.: A method for finding sea breeze days under stable synoptic conditions and its application to the Swedish west coast, International Journal of Climatology, 18, 901–914, https://doi.org/10.1002/(SICI)1097-0088(19980630)18:8<901::AID-JOC295>3.0.CO;2-F, 1998.

480 Bortolotti, P., Tarres, H. C., Dykes, K., Merz, K., Sethuraman, L., Verelst, D., and Zahle, F.: IEA Wind Task 37 on Systems Engineering in Wind Energy – WP2.1 Reference Wind Turbines, Tech. rep., International Energy Agency, https://www.nrel.gov/docs/fy19osti/73492.pdf, 2019.

Brown, A. and Vincent, C.: A daily dataset of sea breeze objects over Australia (1979-2024), https://doi.org/10.5281/zenodo.18012825, 2025.

Brown, A., Short, E., Green, S., and Vincent, C.: sea_breeze: v1.1, https://doi.org/10.5281/zenodo.17220916, 2025a.

485 Brown, A., Vincent, C., and Short, E.: Identifying sea breezes from atmospheric model output (sea_breeze v1.1), EGUsphere [pre-print], 2025, 1–33, https://doi.org/10.5194/egusphere-2025-4848, 2025b.

Cafaro, C., Frame, T. H. A., Methven, J., Roberts, N., and Bröcker, J.: The added value of convection-permitting ensemble forecasts of sea breeze compared to a Bayesian forecast driven by the global ensemble, Quarterly Journal of the Royal Meteorological Society, 145, 1780–1798, https://doi.org/10.1002/qj.3531, 2019.

490 Clarke, R. H.: Fair weather nocturnal inland wind surges and atmospheric bores: Part I Nocturnal wind surges, Australian Meteorological and Oceanographic Journal, 31, 133–145, 1983.

Cowin, E., Wang, C., and Walsh, S. D.: Assessing Predictions of Australian Offshore Wind Energy Resources from Reanalysis Datasets, Energies, 16, https://doi.org/10.3390/en16083404, 2023.

Davidson, M. R. and Millstein, D.: Limitations of reanalysis data for wind power applications, Wind Energy, 25, 1646–1653, https://doi.org/10.1002/we.2759, 2022.

Department of Climate Change, Energy, the Environment and Water: Australia's offshore wind areas, https://www.dcceew.gov.au/energy/renewable/offshore-wind/areas, accessed: 2025-10-13, 2024.

Duffy, P.: turbine-models, [Computer Software] https://doi.org/10.11578/dc.20210112.1, https://doi.org/10.11578/dc.20210112.1, 2020.

Finocchio, P. M., Biernat, K. A., Doyle, J. D., and Reynolds, C. A.: The Influence of Soil Moisture on the Sea Breeze Circulation and the Marine Atmospheric Boundary Layer in Idealized Simulations, Monthly Weather Review, https://doi.org/10.1175/MWR-D-24-0251.1, 2025.

Frysinger, J. R., Lindner, B. L., and Brueske, S. L.: A Statistical Sea-Breeze Prediction Algorithm for Charleston, South Carolina, Weather and Forecasting, 18, 614–625, https://doi.org/10.1175/1520-0434(2003)018<0614:ASSPAF>2.0.CO;2, 2003.

Global Wind Energy Council: Global Wind Report 2025, https://www.gwec.net/reports/globalwindreport, accessed: 10 November, 2025, 2025.

Gorman, N., Haghdadi, N., Bruce, A., and Macgill, I.: NEMOSIS – NEM Open Source Information Service; open-source access to Australian National Electricity Market Data, 2018.

Gunn, A., Dargaville, R., Jakob, C., and McGregor, S.: Spatial optimality and temporal variability in Australia's wind resource, Environmental Research Letters, 18, 114 048, https://doi.org/10.1088/1748-9326/ad0253, 2023.

Huang, Y., Li, S., Zhu, Y., Liu, Y., Hong, Y., Chen, X., Deng, W., Xi, X., Lu, X., and Fan, Q.: Increasing Sea-Land Breeze Frequencies Over Coastal Areas of China in the Past Five Decades, Geophysical Research Letters, 52, https://doi.org/10.1029/2024GL112480, 2025.

Keyser, D., Reeder, M. J., and Reed, R. J.: A Generalization of Petterssen's Frontogenesis Function and Its Relation to the Forcing of Vertical Motion, Monthly Weather Review, 116, 762–781, https://doi.org/10.1175/1520-0493(1988)116<0762:AGOPFF>2.0.CO;2, 1988.

Kraus, H., Hacker, J. M., and Hartmann, J.: An observational aircraft-based study of sea-breeze frontogenesis, Boundary-Layer Meteorology, 53, 223–265, https://doi.org/10.1007/BF00154443, 1990.

Markowski, P. and Richardson, Y.: Air Mass Boundaries, in: Mesoscale Meteorology in Midlatitudes, pp. 115–160, Wiley Online Books, ISBN 9780470682104, https://doi.org/https://doi.org/10.1002/9780470682104.ch5, 2010.

Masouleh, Z. P., Walker, D. J., and Crowther, J. M. C.: A long-term study of sea-breeze characteristics: A case study of the coastal city of Adelaide, Journal of Applied Meteorology and Climatology, 58, 385–400, https://doi.org/10.1175/JAMC-D-17-0251.1, 2019.

Masselink, G. and Pattiaratchi, C. B.: Characteristics of the Sea Breeze System in Perth, Western Australia, and Its Effect on the Nearshore Wave Climate, Journal of Coastal Research, 17, 173–187, http://www.jstor.org/stable/4300161, 2001.

Miao, J. F., Kroon, L. J., de Arellano, J. V.-G., and Holtslag, A. A.: Impacts of topography and land degradation on the sea breeze over eastern Spain, Meteorology and Atmospheric Physics, 84, 157–170, https://doi.org/10.1007/s00703-002-0579-1, 2003.

Miller, S. T., Keim, B. D., Talbot, R. W., and Mao, H.: Sea breeze: Structure, forecasting, and impacts, Reviews of Geophysics, 41, https://doi.org/10.1029/2003RG000124, 2003.

Mulder, F. M.: Implications of diurnal and seasonal variations in renewable energy generation for large scale energy storage, Journal of Renewable and Sustainable Energy, 6, https://doi.org/10.1063/1.4874845, 2014.

Palmer, G., Dargaville, R., Su, C. H., Wang, C., Hoadley, A., and Honnery, D.: Validation of BARRA2 and comparison with MERRA-2 and ERA5 using historical wind power generation, Journal of Southern Hemisphere Earth Systems Science, 75, https://doi.org/10.1071/ES24028, 2025.

Pazandeh Masouleh, Z., Walker, D. J., and Crowther, J. M.: Sea breeze characteristics on two sides of a shallow gulf: Study of the Gulf St Vincent in South Australia, Meteorological Applications, 23, 222–229, https://doi.org/10.1002/met.1547, 2016.

Pettersen, S.: Weather Analysis and Forecasting, Vol. 1, Motion and Motion Systems, McGraw-Hill, 2nd ed. edn., 1956.

Pickering, B., Grams, C. M., and Pfenninger, S.: Sub-national variability of wind power generation in complex terrain and its correlation with large-scale meteorology, Environmental Research Letters, 15, https://doi.org/10.1088/1748-9326/ab70bd, 2020.

Rafiq, S., Pattiaratchi, C., and Janeković, I.: Dynamics of the Land–Sea Breeze System and the Surface Current Response in South-West Australia, Journal of Marine Science and Engineering, 8, 931, https://doi.org/10.3390/jmse8110931, 2020.

Reible, D. D., Simpson, J. E., and Linden, P. F.: The sea breeze and gravity-current frontogenesis, Quarterly Journal of the Royal Meteorological Society, 119, 1–16, https://doi.org/10.1002/qj.49711950902, 1993.

Richardson, D., Pitman, A. J., and Ridder, N. N.: Climate influence on compound solar and wind droughts in Australia, npj Climate and Atmospheric Science, 6, 184, https://doi.org/10.1038/s41612-023-00507-y, 2023.

Richardson, D., Hobeichi, S., Sweet, L.-b., Rey-Costa, E., Abramowitz, G., and Pitman, A. J.: Predicting Australian energy demand variability using weather data and machine learning, Environmental Research Letters, 20, 014 028, https://doi.org/10.1088/1748-9326/ad9b3b, 2025.

Rotunno, R.: On the Linear Theory of the Land and Sea Breeze, Journal of the Atmospheric Sciences, 40, 1999–2009, https://doi.org/https://doi.org/10.1175/1520-0469(1983)040<1999:OTLTOT>2.0.CO;2, 1983.

Short, E., Vincent, C. L., and Lane, T. P.: Diurnal cycle of surface winds in the maritime continent observed through satellite scatterometry, Monthly Weather Review, 147, 2023–2044, https://doi.org/10.1175/MWR-D-18-0433.1, 2019.

Simpson, J. E.: Gravity Currents: In the Environment and the Laboratory., Cambridge university press, 1999.

Simshauser, P. and Wild, P.: Rooftop Solar PV, Coal Plant Inflexibility and the Minimum Load Problem, Energy Journal, 46, 93–118, https://doi.org/10.1177/01956574241283732, 2025.

Soderholm, J., McGowan, H., Richter, H., Walsh, K., Weckwerth, T. M., and Coleman, M.: An 18-year climatology of hailstorm trends and related drivers across southeast Queensland, Australia, Quarterly Journal of the Royal Meteorological Society, 143, 1123–1135, https://doi.org/10.1002/qj.2995, 2017.

Steele, C. J., Dorling, S. R., Von Glasow, R., and Bacon, J.: Idealized WRF model sensitivity simulations of sea breeze types and their effects on offshore windfields, Atmospheric Chemistry and Physics, 13, 443–461, https://doi.org/10.5194/acp-13-443-2013, 2013.

Steele, C. J., Dorling, S. R., Von Glasow, R., and Bacon, J.: Modelling sea-breeze climatologies and interactions on coasts in the southern North Sea: Implications for offshore wind energy, Quarterly Journal of the Royal Meteorological Society, 141, 1821–1835, https://doi.org/10.1002/qj.2484, 2015.

Su, C.-H., Torrance, J., Rennie, S., Howard, E., Stassen, C., Warren, R., Smith, A., Dharssi, I., Pepler, A., Tian, S., Lipson, M., Steinle, P., Franklin, C., Le, T., Wang, C., Masoumi, S., and Marshall, J. L.: The Australian regional atmospheric reanalysis system, version 2 – BARRA2, Journal of Southern Hemisphere Earth Systems Science, 75, https://doi.org/10.1071/ES25032, 2025.

Vincent, C. L. and Dowdy, A. J.: Multi-scale variability of southeastern Australian wind resources, Atmospheric Chemistry and Physics, 24, 10 209–10 223, https://doi.org/10.5194/acp-24-10209-2024, 2024.

Vincent, C. L., Nahar, A., and Say, K.: Wind resources of southeast Australia during peak electricity demand days, Wind Energy Science, 10, 2435–2447, https://doi.org/10.5194/wes-10-2435-2025, 2025.

Virtanen, P., Gommers, R., Oliphant, T. E., Haberland, M., Reddy, T., Cournapeau, D., Burovski, E., Peterson, P., Weckesser, W., Bright, J., van der Walt, S. J., Brett, M., Wilson, J., Millman, K. J., Mayorov, N., Nelson, A. R. J., Jones, E., Kern, R., Larson, E., Carey, C. J., Polat, I., Feng, Y., Moore, E. W., VanderPlas, J., Laxalde, D., Perktold, J., Cimrman, R., Henriksen, I., Quintero, E. A., Harris, C. R., Archibald, A. M., Ribeiro, A. H., Pedregosa, F., van Mulbregt, P., and SciPy 1.0 Contributors: SciPy 1.0: Fundamental Algorithms for Scientific Computing in Python, Nature Methods, 17, 261–272, https://doi.org/10.1038/s41592-019-0686-2, 2020.

Wang, Y., Sabatino, S. D., Martilli, A., Li, Y., Wong, M. S., Gutiérrez, E., and Chan, P. W.: Impact of land surface heterogeneity on urban heat island circulation and sea-land breeze circulation in Hong Kong, Journal of Geophysical Research, 122, 4332–4352, https://doi.org/10.1002/2017JD026702, 2017.

Xia, G., Draxl, C., Optis, M., and Redfern, S.: Detecting and characterizing simulated sea breezes over the US northeastern coast with implications for offshore wind energy, Wind Energy Science, 7, 815–829, https://doi.org/10.5194/wes-7-815-2022, 2022.